Food and Chemical Toxicology 129 (2019) 257–268

Contents lists available at ScienceDirect

Food and Chemical Toxicology

journal homepage: www.elsevier.com/locate/foodchemtox

The hop-derived prenylflavonoid isoxanthohumol inhibits the formation of lung metastasis in B16-F10 murine melanoma model

Tamara Krajnović[a], Dijana Drača[a], Goran N. Kaluđerović[b,1], Duško Dunđerović[c], Ivana Mirkov[a], Ludger A. Wessjohann[b,**], Danijela Maksimović-Ivanić[a], Sanja Mijatović[a,*]

[a] Department of Immunology, Institute for Biological Research "Siniša Stanković", University of Belgrade, Bulevar despota Stefana 142, 11060, Belgrade, Serbia
[b] Department of Bioorganic Chemistry, Leibniz-Institute of Plant Biochemistry, Weinberg 3, D 06120, Halle (Saale), Germany
[c] Institute of Pathology, School of Medicine, University of Belgrade, dr Subotića 1, 11000, Belgrade, Serbia

Keywords:
Isoxanthohumol
Melanoma
Murine metastatic model
Invasion inhibition
Hops flavonoids
Metastasis

A B S T R A C T

Isoxanthohumol (IXN), a prenylflavonoid from hops and beer, gained increasing attention as a potential chemopreventive agent. In the present study, IXN antimetastatic potential *in vitro* against the highly invasive melanoma cell line B16-F10 and *in vivo* in a murine metastatic model was investigated. Melanoma cell viability was diminished in a dose-dependent manner following the treatment with IXN. This decrease was a consequence of autophagy and caspase-dependent apoptosis. Additionally, the dividing potential of highly proliferative melanoma cells was dramatically affected by this isoflavanone, which was in correlation with an abrogated cell colony forming potential, indicating changes in their metastatic features. Concordantly, IXN promoted strong suppression of the processes that define metastasis– cell adhesion, invasion, and migration. Further investigation at the molecular level revealed that the abolished metastatic potential of a melanoma subclone was due to disrupted integrin signaling. Importantly, these results were reaffirmed *in vivo* where IXN inhibited the development of lung metastatic foci in tumor-challenged animals. The results of the present study may highlight the beneficial effects of IXN on melanoma as the most aggressive type of skin cancer and will hopefully shed a light on the possible use of this prenylflavonoid in the treatment of metastatic malignancies.

1. Introduction

Cancer is a clinically challenging disease at a worldwide level, causing more than 7 million deaths annually, with approximately 10 million new diagnoses each year (Anand et al., 2008; Vineis and Wild, 2014). The factors underlying cancer development and progression are extremely complex and only partially understood, and despite the overwhelming efforts in the field of cancer research, some progress achieved in cancer therapy in many instances failed to notably prolong the overall survival rate (Vineis and Wild, 2014). Invasion of neighboring tissues and the establishment of metastatic foci on distant organs represent advanced stages in carcinogenesis and principal features of aggressive malignant phenotype. Dissemination of tumors to distant sites involves a number of consecutive steps which ultimately led to invasion of the target organ where cells integrate and, by communicating with the microenvironment, form metastases (Guan, 2015; Hanahan and Weinberg, 2011). Obstruction of any aspect of metastatic mechanisms could localize the primary tumor and greatly contribute to reducing the risk of cancer-related mortality. Notwithstanding extensive therapeutic protocols, the rates of successful treatments of invasive forms of tumors are still defeatedly low.

Among 100 different types of human cancers known so far (Hanahan and Weinberg, 2011), malignant melanoma is considered to be the most aggressive skin cancer. Even with new therapeutic

Abbreviations: 8-PN, 8-prenylnaringenin; IXN, isoxanthohumol; XN, xanthohumol

* Corresponding author. Department of Immunology, Institute for Biological Research "Siniša Stanković", University of Belgrade, Bul. despota Stefana 142, 11060, Belgrade, Serbia.
** Corresponding author. Dept. Bioorganic Chemistry (NWC), Leibniz Institute of Plant Biochemistry (IPB), Weinberg 3, D-06120, Halle (Saale), Germany.
E-mail addresses: tamara_krajnovic@yahoo.com (T. Krajnović), dracadiana@gmail.com (D. Drača), goran.kaluderovic@ipb-halle.de (G.N. Kaluđerović), drdundjerovic@gmail.com (D. Dunđerović), mirkovi@ibiss.bg.ac.rs (I. Mirkov), wessjohann@ipb-halle.de (L.A. Wessjohann), nelamax@ibiss.bg.ac.rs (D. Maksimović-Ivanić), sanjamama@ibiss.bg.ac.rs (S. Mijatović).
[1] Current address: Department of Engineering and Natural Sciences, University of Applied Sciences Merseburg, Eberhard-Leibnitz-Straße 2, 06217 Merseburg, Germany (goran.kaluderovic@hs-merseburg.de).

https://doi.org/10.1016/j.fct.2019.04.046
Received 22 November 2018; Received in revised form 13 April 2019; Accepted 25 April 2019
Available online 26 April 2019

breakthroughs (Flaherty et al., 2010; Hauschild et al., 2012; Hodi et al., 2010), the median survival rate of patients with metastatic malignant melanoma is estimated at only 6–9 months (Sandru et al., 2014). This type of malignant skin cancer continues to be a challenging disease to treat and there is an urgent need for novel therapeutic strategies.

Whether used as dietary components or plant derivatives, naturally occurring compounds have gained increasing attention as potential chemopreventive agents. (Poly-)Phenolic secondary metabolites comprise one of the largest classes of secondary plant metabolites, with flavonoids being the most attractive among them. Due to their diverse biological properties, prenylated flavonoids have become an important issue in the scientific community nowadays and, thus, are intensively investigated with respect to both their role in nutrition as well as in cancer prevention and therapy (Farag and Wessjohann, 2013; Stevens and Page, 2004; Venturelli et al., 2016). While prenylflavonoids are highly abundant in the hop plant (*Humulus lupulus L.*), the only noteworthy dietary source for humans is beer (Farag et al., 2014, 2012; Stevens and Page, 2004; Venturelli et al., 2016).

Though not as widely studied as xanthohumol (XN), or the strong phytoestrogen 8-prenylnaringenin (8-PN), isoxanthohumol (IXN), a precursor to 8-PN (Wilhelm and Wessjohann, 2006), has received notable attention due to its pharmacological properties. This hop and beer derivative stands out for a diverse spectrum of biological activities, such as proestrogenic, antimicrobial, antioxidant, antiinflammatory and antiangiogenic properties (Jin et al., 2010; Zołnierczyk et al., 2015). The anticancer potential of IXN is noteworthy and it has been acknowledged by a number of *in vitro* studies, including our own (Farag and Wessjohann, 2013; Krajnović et al., 2016). On the other hand, multiple studies showed that IXN evinced none or remarkably low toxic effect on various non-cancerous cells like rat primary hepatocytes, rat intestine epithelial cells (IEC-6), mouse macrophages, mouse embryonic fibroblasts (NIH/3T3), human umbilical vein epithelial cells (HUVEC), human fetal hepatocytes (L-02), human gastric epithelial cells (GES-1), as well as on animal models (Hudcová et al., 2014; Krajnović et al., 2016; Liu et al., 2017; Miranda et al., 1999). Isoxanthohumol (IXN) manifested its antitumor potential through antiproliferative activity against cell lines originating from different types of cancer, e.g. colon, prostate, ovarian, uterine sarcoma, breast, lung, melanoma, glioblastoma, promyelocytic leukemia, acute T lymphocytic leukemia, as well as against some drug-resistant human cancer cells (Allsopp et al., 2013; Delmulle et al., 2008, 2006; Gerhäuser, 2005; Hudcová et al., 2014; Krajnović et al., 2016; Liu et al., 2017; Miranda et al., 1999; Monteiro et al., 2007; Stompor et al., 2017; Tronina et al., 2013; Zołnierczyk et al., 2015). Additionally, it exhibited direct cytocidal effects on some tumor cell lines like B16 and A375 melanoma, CaCo-2 colon and Sk-Br-3 breast cells by cell cycle progression blockade and induction of apoptosis (Allsopp et al., 2013; Krajnović et al., 2016; Monteiro et al., 2007). Recently, our group reported that apoptosis triggered by IXN in B16 and A375 melanoma cells was independent of caspase activation while autophagy played only a cytoprotective role and did not mediate its cytotoxic action (Krajnović et al., 2016). On the other hand, the death of prostate cancer PC-3 and DU145 cells was defined as caspase-independent form of cell death resembling autophagy (Delmulle et al., 2008; Krajnović et al., 2016). Literature data showed that IXN can trigger apoptotic cell death in murine 3T3-L1 mature adipocytes through the mitochondrial pathway as well as inhibit differentiation of preadipocytes (Yang et al., 2007). Furthermore, previous investigations indicate that IXN antitumor potential can be mediated through differentiation of tumor cells as found on colon cancer HT-29 and SW620 cells as well as on melanoma B16 cells (Allsopp et al., 2013; Krajnović et al., 2016; Zołnierczyk et al., 2015). In addition, the loss of “stem” phenotype and pluripotent properties of highly invasive amelanotic A375 cells was confirmed upon the treatment with this isoflavanone (Krajnović et al., 2016). Prenylflavonoids can also affect different types of invasive tumors (Drenzek et al., 2011; Kunnimalaiyaan et al., 2015a, 2015b) in part by disrupting the Wnt signaling pathway whose up-regulation is proven to be associated with metastatic profiles of melanomas (Balint et al., 2005; Borrull et al., 2012; Damsky et al., 2011; Rimm et al., 1999). Likewise, isoxanthohumols’ ability to inhibit invasiveness was seen on HT115 colon cancer cells (Allsopp et al., 2013; Zołnierczyk et al., 2015).

In addition to interfering with the invasion, which greatly characterizes metastasis, IXN has also been proven to inhibit angiogenesis and inflammation and, thus, indirectly exhibits antitumor effects (Bertl et al., 2004a,b; Gerhäuser, 2005; Negrão et al., 2013, 2010). Previously published data discovered that IXN acted as inhibitor/substrate of some efflux drug transporters and therefore had an influence on the applied chemotherapy (Krajnović et al., 2016; Lee et al., 2007; Liu et al., 2017; Tan et al., 2014).

Unfortunately, the findings about the *in vivo* effectiveness of hops prenylflavonoids against tumors are still scarce. So far, only few studies on animal models have dealt with this topic (Benelli et al., 2012; Liu et al., 2015; Monteiro et al., 2008; Venè et al., 2012). Nonetheless, *in vivo* investigations can provide valuable information about the compounds actual properties and are of exceptional importance for each forthcoming drug development.

In the present study, antimetastatic properties of the hop prenylflavonoid IXN have been investigated for the first time. It was found that IXN induced combined cell death by caspase-dependent apoptosis as well as autophagy. Aside from affecting the dividing potential of the highly invasive melanoma cell line B16-F10, IXN, to a great extent, suppressed their ability to adhere, migrate, and invade. Additionally, the integrin signaling pathway, which is essential to metastatic processes, was thoroughly evaluated, giving an insight into the intracellular background of IXN mode of action. Importantly, the present paper also focuses on the antimetastatic potential of IXN *in vivo*.

2. Materials and methods

2.1. Reagents, cells and animals

Cell culture medium RPMI-1640 was purchased from Biowest (Riverside, MO, USA). Fetal bovine serum (FBS), phosphate-buffered saline (PBS), trypsin, dimethyl sulfoxide (DMSO), crystal violet (CV), carboxyfluorescein diacetate succinimidyl ester (CFSE) were bought from Sigma Aldrich (St. Louis, MO, USA). 3-(4,5-dimethythiazol-2-yl)-2,5-diphenyltetrazolium bromide (MTT), bovine serum albumin (BSA) and Tween® 20 were obtained from AppliChem (St. Louis, MO, USA). Paraformaldehyde (PFA) was purchased from Serva (Heidelberg, Germany). Annexin V-FITC (AnnV) was from BioLegend (San Diego, CA, USA) and propidium iodide (PI) was from BD Pharmingen (San Diego, CA, USA). ApoStat was purchased from R&D Systems (Minneapolis, MN, USA) and acridine orange (AO) was from Labo-Moderna (Paris, France). Matrigel® was bought from BD Bioscience (Bedford, MA, USA). Isoxanthohumol (IXN) was obtained from Orgentis (Gatersleben, Germany). The murine metastatic melanoma B16-F10 cell line was a kind gift from Prof. Barbara Seliger (Institute for Medical Immunology, Martin Luther University Halle-Wittenberg, Germany).

Cells were cultivated and routinely propagated in HEPES-buffered RPMI-1640 culture medium supplemented with 10% heat-inactivated FBS, 2 mM L-glutamine, 0.01% sodium pyruvate, penicillin (100 units/mL) and streptomycin (100 μg/mL) at 37 °C in a humidified atmosphere with 5% CO_2. For viability determination, cells were seeded at 5×10^3 cells/well in 96-well plates, for flow cytometry and immunoblot analysis at 2.5×10^5 cells/well in 6-well plates, for cell survival clonogenic assay at 1×10^3 cells/well in 6-well plates, for adhesion assay at 3×10^4 cells/well in 96-well plates and for migration and invasion assays at 2×10^5 cells/well in 24-well plates.

Animals used in this study were female inbred C57BL/6 mice obtained from the facility of the Institute for Biological Research “Siniša Stanković”, University of Belgrade (Belgrade, Serbia). Animals were kept under the standard laboratory conditions (non-specific pathogen

free) with *ad libitum* regime of food and water intake. The handling of animals and the study protocols were in agreement with the rules of the European Union and were approved by the Institutional Animal Care and Use Committee at the Institute for Biological Research "Siniša Stanković", University of Belgrade (07–10/15).

2.2. Preparation of drug solution

Isoxanthohumol was dissolved in DMSO at 100 mM concentration and stored at −20 °C according to the manufacturers' instructions. Working solutions were prepared by thawing and shaking the stock solution and by making dilutions with culture medium or PBS before *in vitro* or *in vivo* treatment, respectively. When different concentrations were used, DMSO was added to control cultures in the concentration found in the highest final concentration of IXN, to assure equal DMSO content.

2.3. Cell viability evaluation by MTT and CV assays

B16-F10 cells were treated with a wide range of concentrations (1.6–100 μM) of IXN for 48 h. The estimation of viability was done by MTT and CV assays. In order to conduct MTT test, cells were incubated with MTT solution (0.5 mg/mL) at 37 °C for approximately 1 h which was followed by the removal of the dye. Formed formazan crystals were dissolved in DMSO. For the CV test, attached viable cells were fixed with 4% PFA for 10 min at room temperature (RT) and subsequently stained with 2% CV solution for 15 min. Further, cells were washed with tap water, air-dried and the dye was then dissolved in 33% acetic acid. The absorbance of both dissolved dyes was measured with an automated microplate reader at 570 nm with a reference wavelength of 670 nm. Cell viability is expressed as a percentage of control values (untreated cells), which was set to 100%.

2.4. Annexin V-FITC/PI, ApoStat and acridine orange staining

In order to detect apoptosis, autophagy and caspase activity, B16-F10 cells were exposed to an IC_{50} dose (30 μM) of IXN for 48 h. For apoptosis detection, cells were stained with AnnV/PI solution for 15 min at RT in the dark, according to the manufacturers' instructions. For the determination of IXN influence on caspase activity, cells were stained with ApoStat solution in PBS-5% FBS for 30 min at 37 °C, washed and resuspended in PBS. AO staining of the cells considered incubation with the dye in a final concentration of 10 μM in PBS at 37 °C for 15 min, washing, and resuspending in PBS. All cell samples were analyzed with BD FACSAria™ III Cell Sorter, using the BD FACSDiva™ software (BD Biosciences, San Jose, CA, USA).

2.5. CFSE staining

To measure the influence of IXN on the proliferation rate, cells were prestained with 1 μM CFSE in PBS-0.1% FBS for 10 min at 37 °C prior to their cultivation in the presence of an IC_{50} dose (30 μM) of IXN for 48 h. Subsequently, cells were washed, trypsinized, and resuspended in PBS. Results were obtained from the analysis of cell samples with BD FACSDiva™ software on a BD FACSAria™ III Cell Sorter.

2.6. Cell clonogenic survival assay

The colony forming capacity of B16-F10 cells was evaluated *in vitro* using a clonogenic test. Cells, maintained as monolayers in 75 cm^2 tissue culture flasks, were treated with an IC_{25} dose (15 μM) of IXN for 48 h. At the end of the incubation period, cells were trypsinized, counted, reseeded in 6-well plates, and allowed to grow in a humidified 5% CO_2 environment at 37 °C for 7 days for colony formation. The culture medium was changed on day 4. After 7 days of cultivation, the culture medium was removed; colonies were washed with PBS and fixed with 4% PFA for 30 min at RT. The fixed cell colonies were then stained with 2% CV solution for 15 min at RT. Finally, the cells were washed twice with PBS and colonies with more than 50 cells formed from one cell were photographed under the light microscope equipped with a camera. Digital images of the colonies obtained by a camera served for quantitative evaluation of colony forming capacity which was performed by means of imaging analysis software package ImageJ. The average colony count of three wells was used to calculate plating efficiency and surviving fraction. Plating efficiency (PE) was calculated as a number of colonies counted/number of cells plated × 100, while the surviving fraction was calculated as PE of treatment/PE of control × 100.

2.7. Cell matrix adhesion assay

Tumor cell adhesion was assayed using 96-well plates which were precoated with 20 μg/mL reconstituted basement membrane (Matrigel®) and left at 4 °C overnight for gelling. B16-F10 cells were grown in 75 cm^2 tissue culture flasks and pretreated for 48 h with an IC_{25} dose (15 μM) of IXN. After the treatment period had expired, cells were detached, collected, and left for approximately 30 min at RT for membrane reconstitution. The wells were washed with PBS before seeding the cells and allowing them to adhere to Matrigel® for 1 h at 37 °C. Nonadherent cells were then rinsed with PBS while the cells remaining attached were fixed with 4% PFA and stained with 2% CV solution for 15 min at RT. Afterwards, cells were washed with tap water and the dye was solubilized with 33% acetic acid. Relative cell adhesion was quantified by monitoring the absorbance of the dye at 570 nm with a reference wavelength of 670 nm. The results are calculated as the percentage of control (untreated cells).

2.8. Wound healing assay

Cell motility was investigated *in vitro* by a wound healing assay, in which cells migrate bidirectionally from the edges of a scratch wound. For the purpose of a scratch assay, B16-F10 cells were firstly allowed to grow to 80% confluent monolayers in 6-well plates. The migration was initiated by a sterile pipette tip which was drawn across the center of the wells to produce a clean wound area. The wounded cell layers were washed twice with fresh PBS to remove loose or damaged cells. Cells were further incubated at 37 °C for 48 h with or without $IC_{12.5}$ (7.5 μM) and IC_{25} (15 μM) doses of IXN. At the end of the incubation period, cells were washed, fixed with 4% PFA for 10 min and stained with 2% CV solution for 1 min at RT. The wounds were observed under a microscope and digitally photographed.

2.9. Transmigration and invasion assays

To quantitatively evaluate the effect of IXN on *in vitro* migration and invasion potential of B16-F10 cells, the transmigration and invasion assays were used as previously described (Mojic et al., 2012). In brief, Transwell inserts (8-μm pore size transparent PET membrane cell culture inserts; BD Bioscience, Bedford, MA, USA) assembled in 24-well plates were used. For invasion assay, the upper surfaces of the Transwell membranes were precoated with a layer of Matrigel® (0.5 mg/mL in PBS; 10 μL/membrane) and left at 4 °C overnight for gelling, whereas for migration assay membranes remained uncoated. The inserts with Matrigel® were washed twice with PBS before seeding the cells. After a 48 h-long incubation period with an IC_{25} dose (15 μM) of IXN, cells were harvested, collected, resuspended in 0.1% BSA-RPMI 1640 medium and carefully seeded into the upper compartment of each insert. The lower chambers were filled up with 10% FBS-RPMI 1640 medium which served as chemoattractant for the cells. The plates were then incubated at 37 °C for 12 h, allowing the cells to invade through the Matrigel®-coated membranes, and for 24 h for the migration assay. The non-invaded/migrated cells which remained on the upper surfaces

of the filters were carefully removed with a cotton swab while the invading/migrating cells on the lower side of the membranes were fixed with 4% PFA for 10 min and stained with Mayer's hematoxylin (BioOptica; Milan, Italy) for 3 min at RT. In the end, the cells were washed with tap water and air-dried before Transwell membranes were cut out of inserts and mounted on glass slides. Invading/migrating cells were counted manually by three different persons under the light microscope at 40 × magnification. The average number of cells in 5 randomly selected and independent fields per membrane is presented. Each experiment was performed in triplicate.

2.10. Western blot analysis

B16-F10 cells were cultivated in the presence of an IC_{50} dose (30 μM) of IXN for 2, 6, 24 and 48 h and subsequently lysed in protein lysis buffer (62.5 mM Tris-HCl pH 6.8, 2% w/v SDS, 10% glycerol, 50 mM dithiothreitol). The electrophoretic separation of proteins was performed on 10–12% SDS-polyacrylamide gels while a PageRuler prestained ladder (Thermo Fisher Scientific; Waltham, MA, USA) was used as protein molecular weight marker. Proteins were then transferred to polyvinylidenedifluoride membranes at 5 mA/cm^2 using a semidry blotting system (Fastblot B43, BioRad; Göttingen, Germany). Blocking of membranes was done with 5% (w/v) BSA in PBS-0.1% Tween 20. Membranes were incubated overnight at 4 °C with specific primary antibodies to Vinculin, FAK, α-Smooth Muscle Actin (Sigma Aldrich; St. Louis, MO, USA), Integrin alpha 6, Rho (Y486), β-Actin (Abcam; Cambridge, UK) and α-Tubulin (11H10) (Cell Signaling Technology; Danvers, MA, USA). Goat anti-rabbit IgG-HRP (Cell Signaling Technology; Danvers, MA, USA) and goat anti-mouse IgG-HRP (Santa Cruz Biotechnology; Dallas, TX, USA) were used as secondary antibodies. Bands were visualized by a chemiluminescence detection system (ECL, GE Healthcare; Chalfont St. Giles, Buckinghamshire, UK).

2.11. Induction of lung metastasis and in vivo treatment

For evaluation of IXN metastatic potential *in vivo*, B16-F10 cells were grown to 80% confluence, then trypsinized, resuspended in PBS and 200 μL of cell suspension (5×10^5) was intravenously injected into the tail vein of 2.5 month-old female syngeneic C57BL/6 mice. The mice were left to develop lung metastases for three days. On the third day following cell inoculation, the animals were randomly allocated to two groups of eight and were treated daily with IXN (20 mg/kg in 2% DMSO-PBS) or vehicle solution (2% DMSO-PBS) for 18 consecutive days. Mice were euthanized by CO_2 asphyxiation on day 21 after cell implantation and lungs with metastases were extracted from each animal under sterile conditions. Organs were bleached in 3% H_2O_2 and washed in PBS before being digitally photographed with a camera. Additionally, the number of lung nodules was counted by four different persons, and the lungs were prepared for further histology experiments. Before cell inoculation and on day 21 after cell inoculation, urine from the animals was collected and biochemical parameters were analyzed with Multistix 10 SG (Bayer; Leverkusen, Germany). The weights of animals and their viability were monitored regularly during the entire experiment.

2.12. Histology

In order to perform rapid microscopic analyses of specimens, a frozen section procedure was used. Surgically removed lung specimens from 8 different animals from each group were bleached in 3% H_2O_2 and washed in PBS. Isolated lungs with metastases were then fixed in 4% PFA for 24 h at 4 °C after which they were transferred into 30% sucrose solution and left for 7 days at 4 °C, followed by embedding. Using a cryostat, tissues embedded within Tissue-Tek® O.C.T. medium (Sakura Finetek; Torrance, CA, USA) were cut frozen into 14 μm-thick cryosections and picked up on glass slides for hematoxylin and eosin staining. In brief, cryosections were stained with filtered Mayer's hematoxylin for 4 min, washed with tap water and counterstained with eosin for 3 min at RT. The excess stain was removed by shortly rinsing with tap water. Dehydration was achieved by immersion in a series of increasing concentrations of alcohol after which two changes of xylene were used for clearing. Further, glass slides were mounted with DPX mounting medium (Thermo Scientific; Waltham, MA, USA), observed and digitally photographed under a DM RB Photomicroscope (Leica; Wetzlar, Germany) with a DFC 320 CCD Camera (Leica) at 5 × magnification.

2.13. Immunohistochemistry and immunofluorescence

Isolated lungs of animals with metastases were alternatively fixed in 4% formalin for 24 h and processed for conventional 4 μm-thick paraffin wax sections. The sections were further dewaxed, rehydrated in a series of decreasing concentrations of alcohol and antigen retrieval was done by cooking in a microwave oven for 20 min in citrate buffer pH 6. Inactivation of endogenous peroxidases was done with 3% H_2O_2 in 10% methanol in 0.5% Triton X-100-PBS while 10% FBS-PBS was used to block nonspecific background staining. Incubation with specific primary antibodies to HMGB1 (GT383) (Thermo Fisher Scientific; Waltham, MA, USA) and anti-S100 (4B3) (Abcam; Cambridge, UK) at dilution 1:100 was done at RT for 1 h. For the detection of HMGB1 primary antibody, Primary Antibody Enhancer and Large Volume HRP Polymer from Lab Vision™ UltraVision™ LP Detection System: HRP Polymer/DAB Plus Chromogen were used while secondary Lab Vision™ Biotinylated Goat anti-Polyvalent (Ready-To-Use) antibody and tertiary Lab Vision™ Ready-To-Use Streptavidin Peroxidase antibody (Thermo Fisher Scientific; Waltham, MA, USA) were employed for the detection of primary anti-S100 antibody. Each of them was applied for 10 min at RT. Between all steps, sections were immersed in PBS 3 × 5 min. 3,3′-diaminobenzedine (DAB, Dako North America; Carpinteria, CA, USA) was used as a detection reagent and sections were counterstained with Mayer's hematoxylin. Further, glass slides were mounted and analyzed under Olympus BX50 microscope (Olympus, Tokyo, Japan) with Olympus DP70 camera at 200 × magnification.

For detection of Ki-67 protein expression, immunofluorescent staining was done. After the antigen retrieval and blocking procedure, the sections were incubated with FITC conjugated Ki-67 (M-19) antibody (Santa Cruz Biotechnology; Dallas, TX, USA) diluted 100 times at 4 °C overnight. After washing in PBS, the slides were mounted with DAPI Fluoromount-G® (Southern Biotech; Birmingham, AL, USA) and analyzed with Zeiss AxioObserver Z1 inverted fluorescence microscope (Carl Zeiss AG, Oberkochen, Germany) at 200 × magnification.

2.14. Statistical analysis

The results are presented as means ± SD of triplicates from one representative of three repeated experiments with similar results. The significance of the differences between various treatments was determined by variance analysis (ANOVA), followed by a Student-t test. A p value less than 0.05 was considered significant.

3. Results

3.1. IXN induced programmed cell death type I and II in metastatic B16-F10 cells

It was previously reported that IXN could successfully decrease the viability of mouse melanoma B16 and human melanoma A375 cells. To evaluate the influence of the compound on the viability of a metastatic clone, B16-F10 cells, a wide range of concentrations was applied for 48 h and the survival of cells was analyzed by MTT and CV tests. As found previously, IXN dose-dependently decreased the viability of cells

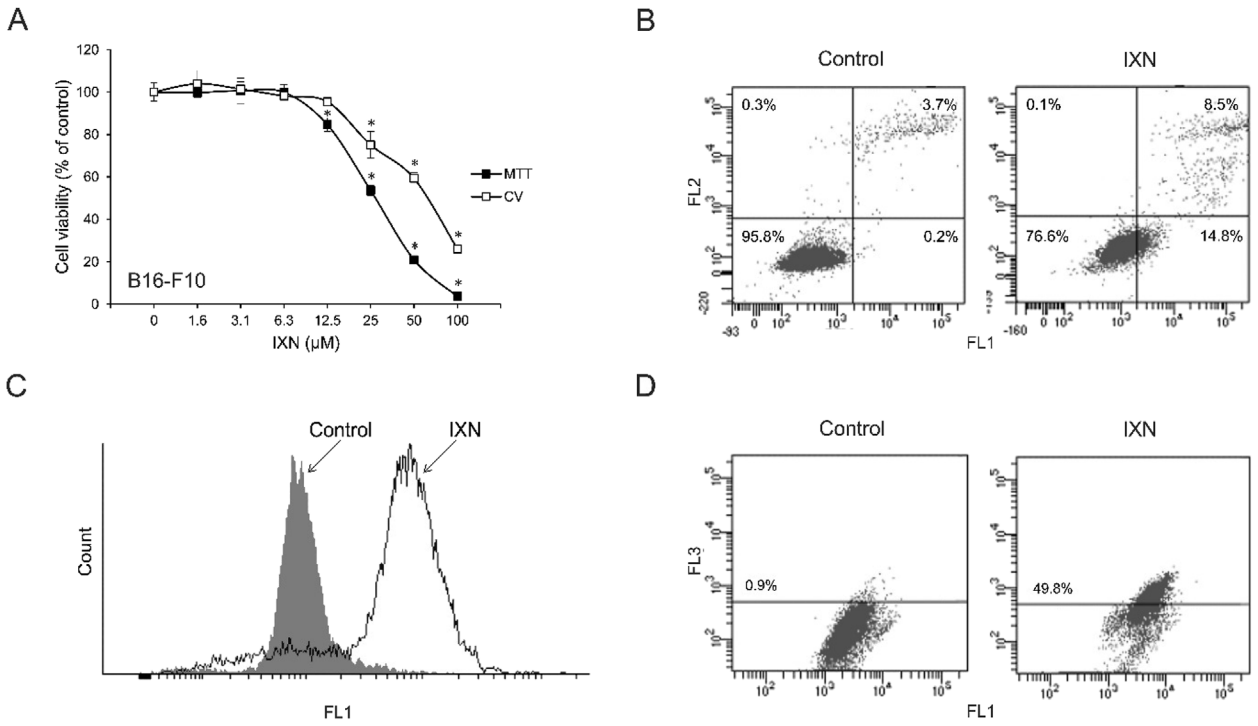

Fig. 1. IXN suppresses the growth of B16-F10. Cells (5×10^3 cells/well) were treated with IXN in a concentration series (1.6–100 μM) for 48 h and the number of viable cells was determined by MTT and CV assays. The cell viability is expressed as a percentage of control values (untreated cells), and the data are presented as mean ± SD from three independent experiments (A). Ann/PI staining of cells exposed to IC_{50} dose (30 μM) of IXN (B), ApoStat (C), and AO staining (D), all performed after 48 h of treatment and subsequently analyzed by flow cytometry. Dot plots and histogram are representative ones selected from three repeated experiments. *$p < 0.05$ refers to untreated cultures.

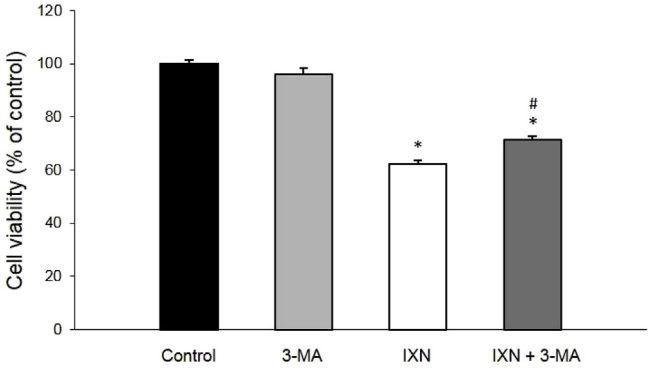

Fig. 2. IXN promotes autophagic cell death. B16-F10 cells (5×10^3 cells/well) were exposed to an IC_{50} dose (30 μM) of IXN and 3-MA (in final concentration of 1 mM) for 48 h. Cell viability was determined by MTT test and expressed as a percentage of control values (untreated cells). The data are presented as mean ± SD obtained from three independent experiments. *$p < 0.05$ refers to untreated cultures; #$p < 0.05$ refers to IXN treated cultures.

with the IC_{50} dose of 30 μM and 42 μM obtained by MTT and CV assays, respectively (Fig. 1A). The IC_{50} value calculated by MTT test was lower, indicating that the drug affected mitochondrial respiration prior to cell death. To further define the mechanism of IXN action, double staining Ann/PI was performed. The 48 h-lasting treatment with IXN elevated the percentage of both, early (Ann^+PI^-) and late (Ann^+PI^+) apoptotic cells (Fig. 1B). In parallel, a remarkable activation of caspases was determined after the same period of incubation, suggesting that apoptosis was probably realized through typical pathways (Fig. 1C). On the other hand, the intensified presence of autophagosomes upon the exposure of cells to IXN revealed an enhanced autophagic process (Fig. 1D). To define the role of detected autophagy, cells were cotreated with 3-methyladenine (3-MA). This compound works through a blockade of the autophagosome formation by the inhibition of type III phosphatidylinositol 3-kinases. The viability of cells exposed to IXN in the presence of 3-MA was 10% higher in comparison to IXN alone (Fig. 2). It is clear that the inhibition of autophagy can partly neutralize the activity of IXN, hence both, caspase-dependent apoptosis and autophagic cell death contribute to IXN promoted cell viability decrease.

3.2. IXN abrogated B16-F10 cells metastatic potential

The principal feature of the aggressive malignant phenotype is its potential to form metastases. Since B16-F10 cells are highly proliferative, their potential to divide in the presence of the experimental therapeutic was the first to elaborate. In comparison to untreated cultures, 48 h-long incubation with IXN resulted in suppressed proliferation (Fig. 3A). While almost 91% of control cells were divided during the indicated time interval, 88.7% of IXN treated cells were blocked. Accordingly, the ability of cells to form colonies was dramatically abrogated after their exposure to IXN compared to control cultures where the rapid proliferation manifested through formation of numerous, spacious colonies observed (Fig. 3B). To exclude the possibility that the antimetastatic effect of IXN may be due to its cytocidal activity, all following experiments were done with IC_{25} dose or even lower. The clonogenic survival fraction in IXN exposed cultures was reduced by more than 60%. The colony forming potential correlated with diminished proliferating ability of treated cells indicating changed metastatic features of B16-F10 cells. To confirm this, cell adhesion, migration, and invasion were assessed. For that purpose, cells were pretreated with an IC_{25} dose of IXN for 48 h before the analyses. Since cell adhesion is a pivotal step in a cascade of events characteristic for metastatic processes, the influence of IXN on the cell ability to adhere to plastic and extracellular matrix was analyzed– using Matrigel® for the latter. Cultivation in the presence of IXN decreased adhesion of plated cells to

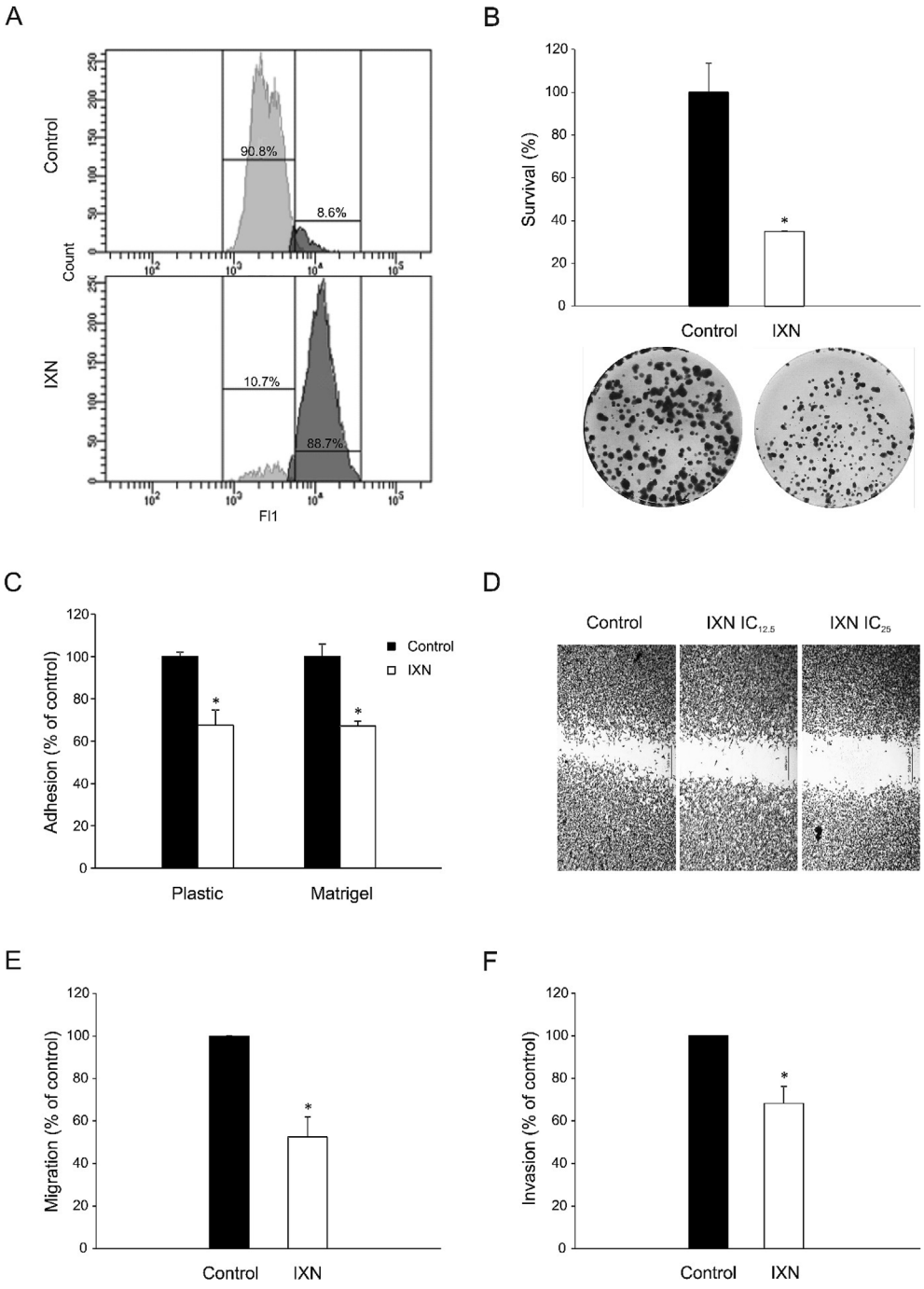

Fig. 3. IXN abrogates B16-F10 proliferation and metastatic features. Cells were exposed to an IC_{50} dose (30 μM) of IXN. CFSE staining followed by flow cytometry was done after 48 h and a representative histogram from three repeated experiments is presented (A). Cells were pretreated with an IC_{25} dose (15 μM) of IXN for 48 h and a clonogenic survival assay was done after 7 days of cultivation (B). Cells were exposed to IC_{25} dose (15 μM) of IXN for 48 h and adhesion (C), wound healing (D), migration (E), and invasion (F) were analyzed as indicated in material and methods section. Results (B, C, E, and F) are expressed as a percentage of control values (untreated cells) and are presented as mean ± SD obtained from three repeated experiments. *$p < 0.05$ refers to untreated cultures.

both surface types to a similar extent, indicating a general loss or blockage of adhesive molecules (Fig. 3C). The next step associated with metastasis was defined by the cell migratory profile. To avoid a contribution of the drugs' cytotoxicity, a 48 h-wound healing test was done with the doses that were two or four times lower than the IC_{50} dose. Compared to a control culture where the gap between cells was almost completely bridged, IXN treatment at both, IC_{25} and $IC_{12.5}$ doses remarkably reduced the cells' ability to fill wounded area (Fig. 3D). It was clear that the motility of cells was affected by the drug. Furthermore, using a Boyden-chamber we found that IXN, even if applied at a subtoxic dose, weakened the migration of cells through 8 μm pores. The migration of treated cells was reduced by approximately 50% compared to the control (Fig. 3E). Accordingly, their ability to pass the barrier made of the reconstituted basement membrane was 40% lower than that of untreated cells (control). This shows that IXN is able to significantly decrease migration, invasion, and adhesion of B16-F10 cells (Fig. 3F).

3.3. IXN-diminished metastatic potential is due to disrupted integrin signaling

It is well documented that tumor invasiveness and migratory potential of cells depend on engagement of integrin receptors and the propagation of downstream signal. Integrin receptors and actin are connected through adaptor proteins (talin, vinculin, α-actinin, etc.), Arp2/3 complex, kinases (FAK, ILK, etc.) and small G-proteins (Rho GTPases) (Nagano et al., 2012). To delineate the interference of IXN with selected proteins important for the integrin-triggered rearrangement of the cytoskeleton, cells were exposed to IC_{50} dose of IXN and protein expressions were analyzed at time intervals indicated in Fig. 4.

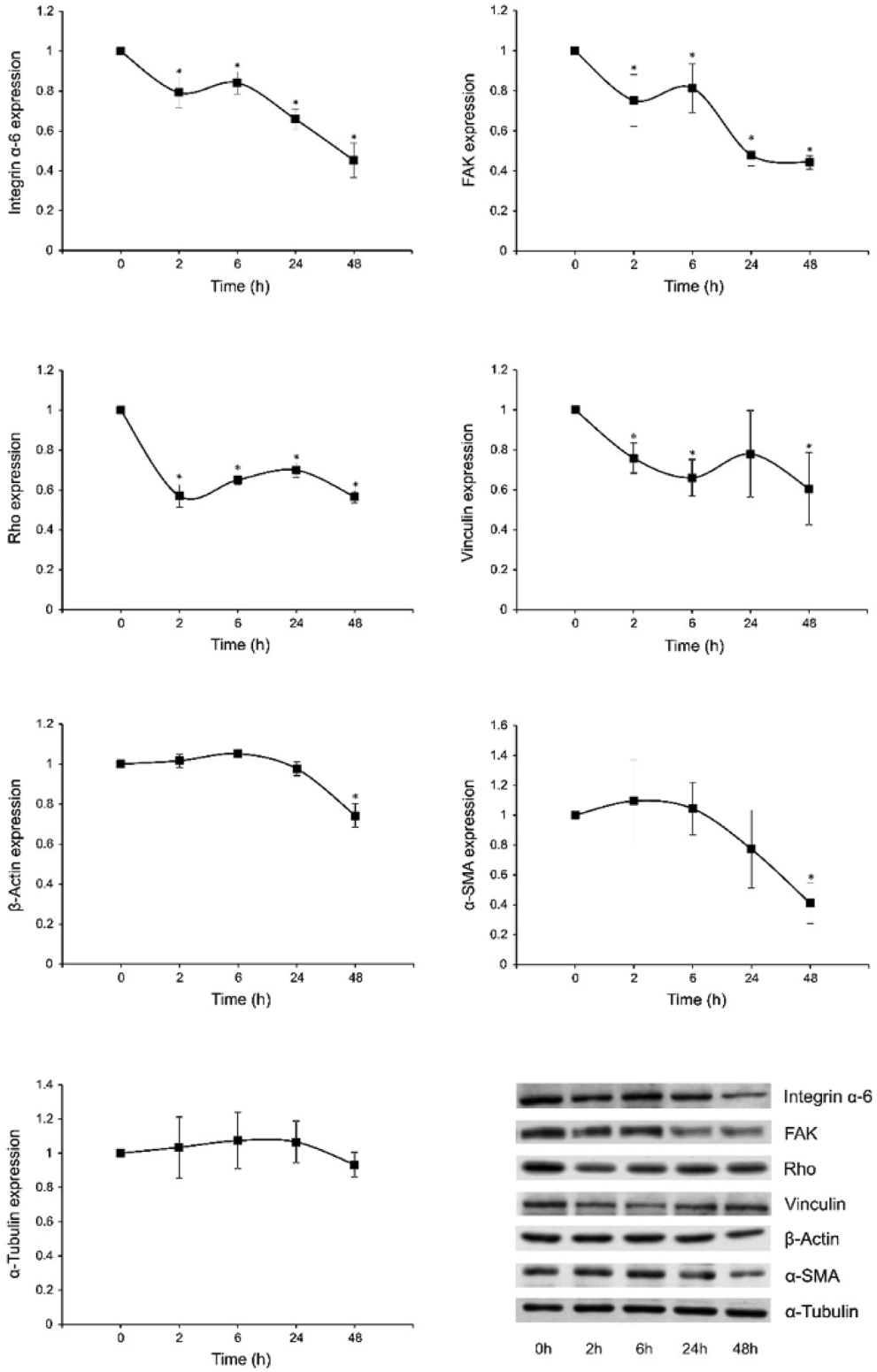

Fig. 4. IXN interrupts the integrin signaling pathway. B16-F10 cells were exposed to an IC_{50} dose (30 μM) of IXN and protein expressions were analyzed by Western blot at indicated time points. α-Tubulin served as a reference. The data are presented as mean ± SD calculated from densitometric analysis of three independent experiments. *$p < 0.05$ compared to untreated cultures.

Since the expression of α-Tubulin was not affected by the treatment at any time point, it served as reference. Integrin α-6 and subsequently the expressions of FAK, vinculin, and Rho kinase were remarkably down-regulated in the presence of IXN (Fig. 4). In addition, the expression of α-smooth muscle actin, a protein characteristic for an aggressive phenotype, was also diminished after the treatment. Finally, β-Actin whose abnormal expression and polymerization are associated with the invasiveness and metastasis of different types of cancer, was also decreased at the final measurement time point. Altogether, it is evident that IXN affects the adhesion and migratory potential of the metastatic

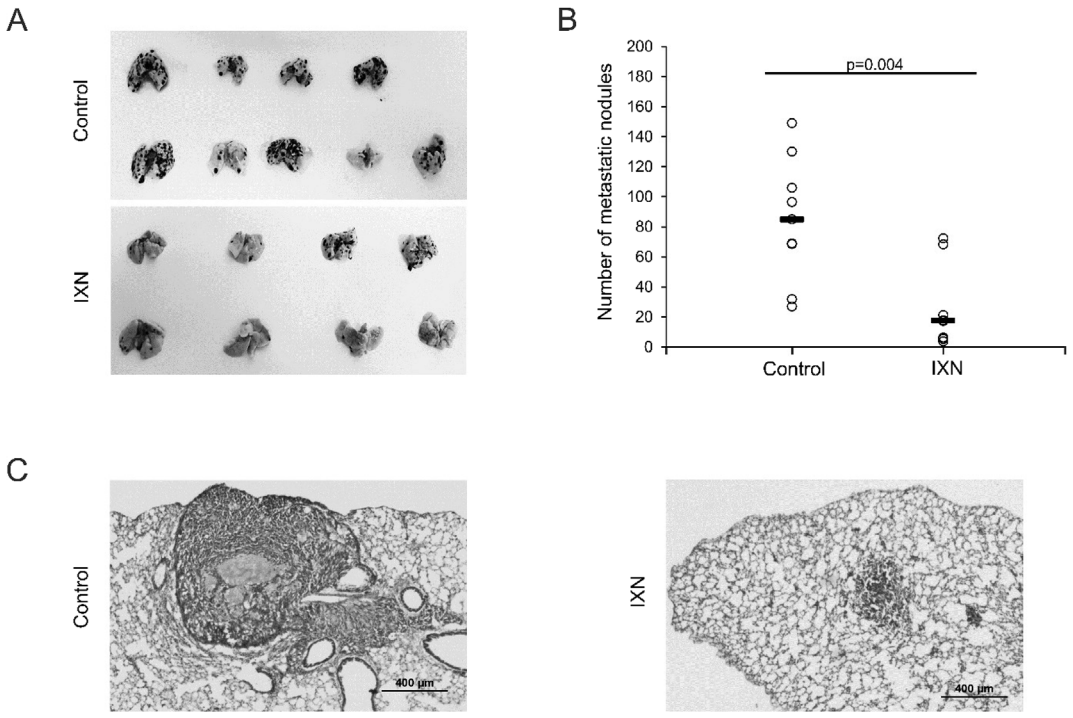

Fig. 5. IXN suppresses the development of lung metastasis. B16-F10 cells (5×10^5) were inoculated into the tail vein of C57BL/6 mice. Animals were treated with 20 mg/kg IXN daily for 18 consecutive days and the number of metastases was determined after 21 days (A, B). Microscopic evaluation of lung cryosections at 5 × magnification, scale bar – 400 µm. Representative images of lung cryosections for each group are presented (C).

skin melanoma B16-F10 subclone by compromising integrin mediated signaling.

3.4. IXN inhibited lung metastasis formation in vivo

To determine the antimetastatic potential of IXN against the metastatic clone F10 of B16 melanoma *in vivo*, a tail vein metastasis model was employed. Cells were administered by intravenous injection, and after 3 days, the daily treatment with 20 mg/kg IXN started and was administrated for 18 successive days. The dose used was already found efficient in a solid melanoma model C57BL/6 mice (Krajnović et al., 2016). The duration of treatment was defined by the fact that the chosen period was optimal for metastasis development following the induction of the disease by a certain number of melanoma cells (Ortiz et al., 2016). On day 21, the animals were sacrificed and lungs were estimated for metastatic nodules presence. As presented in Fig. 5A and B, in the IXN treated group only in two of eight animals the number of metastatic foci was in the range of values observed for the control group. Lungs of the other 6 animals showed significantly fewer metastases. The difference in number of metastatic nodules was accompanied by a reduced diameter per nodule in the IXN treated group (Fig. 5C). Moreover, a rich vascularization of metastatic foci was found in the control group while for the IXN treated animals this was not observed.

The decreased number and diameter of metastatic foci was followed by changes in the expression of specific proteins reflecting their metastatic features. As presented in Fig. 6, HMGB1 expression in nuclei of lung metastatic cells upon the treatment of animals with IXN was remarkably diminished in comparison to the control animals indicating decreased malignant potential of these cells. On the other hand, enhanced expression of S100 protein in lung cellular deposits accompanied by the acquisition of spindle shape and low expression of proliferative marker Ki-67 confirmed the differentiation of metastatic cells toward less invasive phenotype in response to IXN treatment (Fig. 6). Importantly, no signs of toxicity were detected after application of IXN, based on indicators such as general discomfort, impaired movement, changed behavior, hair loss, weight changes, or diarrhea. In addition, the absence of IXN toxicity was confirmed at the biochemical level. In fact, biochemical parameters from urine were the same after 21 days upon disease induction (see Suppl. Table 1). Taken together, it is obvious that IXN possesses a strong antimetastatic potential.

4. Discussion

Malignant melanoma is the most aggressive form of melanoma tumor for which therapeutic options are quite limited. The median survival for patients with metastases is about 6–9 months, so the evaluation of new antimelanoma agents is still an attractive field (Sandru et al., 2014). In the present study, the antimetastatic properties of the prenylated flavonoid IXN on the highly invasive melanoma cell line B16-F10 developed from the parental B16 cells through the successive transfer of tumor cells isolated from lung metastasis in 10 repeated cycles were presented (Danciu et al., 2013). Exposure of B16-F10 cells to IXN resulted in combined cell death induction– by apoptosis and autophagy. This is consistent with previous findings about the antitumor potential of IXN on other cell lines originating from different types of tumors (Allsopp et al., 2013; Delmulle et al., 2008; Krajnović et al., 2016; Monteiro et al., 2007). It was found that IXN induced apoptosis on B16, A375 melanoma, Sk-Br-3 breast, and Caco-2 colon cancer cells while the death of prostate cancer PC-3 and DU145 cells was more similar to autophagy (Allsopp et al., 2013; Delmulle et al., 2008; Krajnović et al., 2016; Monteiro et al., 2007). It was previously reported that apoptosis triggered in B16 cells was independent of caspase activation (Krajnović et al., 2016). On its metastatic counterpart, B16-F10, we detected an intensified caspase activity that might be due to a different role of this enzyme family in the processes connected with cancer. Namely, it is known that caspases are not only important for apoptotic program execution but also play significant roles in other numerous processes such as phenotype transformation, apoptosis/autophagy interplay as well as intercellular communication (Shalini et al., 2015). This is not the only point where less vs. more invasive forms of cancer can show a diverse response to IXN. In addition, IXN treatment

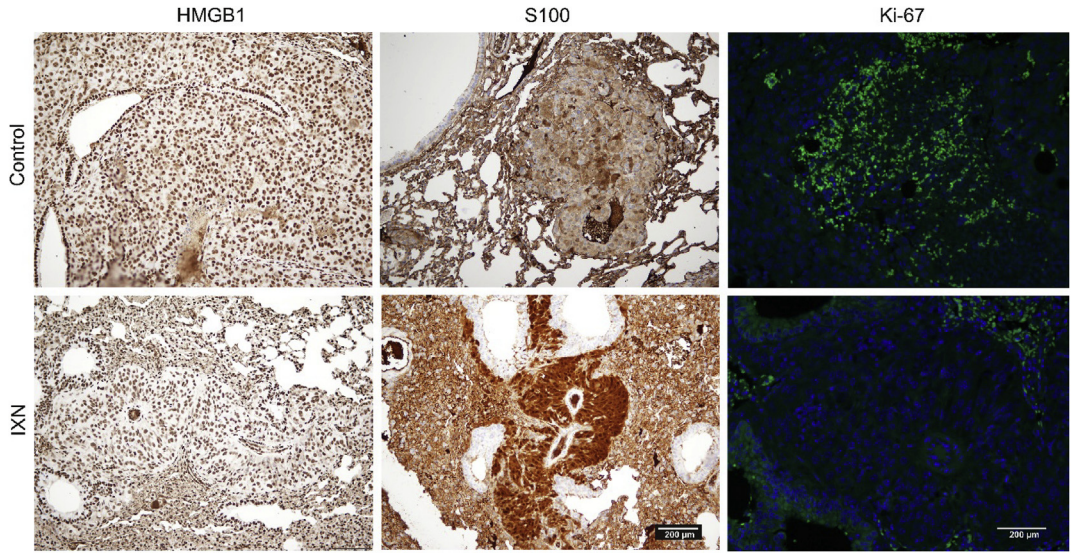

Fig. 6. IXN affects metastatic cells phenotype. B16-F10 cells (5×10^5) were inoculated into the tail vein of C57BL/6 mice. Animals were treated with 20 mg/kg IXN daily for 18 consecutive days and the expression of molecular markers was evaluated on paraffin-embedded sections of lungs. HMGB1 and S100 expressions were evaluated by light microscopy at 200 × magnification (scale bar – 200 µm), while Ki-67 expression was analyzed by fluorescent microscopy at 200 × magnification (scale bar – 200 µm). Representative images of lung sections for each group are presented.

appears to exert destructive autophagy in B16-F10 cells while in less invasive phenotype the opposite behavior was observed (Krajnović et al., 2016). Accordingly, inhibited proliferation accompanied by changes in the motility of metastatic cells was detected. CFSE staining and a clonogenic assay clearly showed that the dividing potential of cells recognized as highly proliferative was diminished under IXN treatment. Danciu et al. found that the doubling time of the B16-F10 subclone was lower than that of its less aggressive counterpart (Danciu et al., 2013), and that sublines of B16 cells, B164A5, B16GMCSF, B16FLT3, and B16-F10 had dissimilar intracellular features and responses to the same stimuli. Therefore, it is not surprising that B16-F10 cells express different pathways in cell death realization upon the same stimuli. Often, decreased proliferation coincides with a loss of malignant potential. In general, it is considered that tumor dissemination to distant sites includes a cascade of events, starting from primary tumor neovascularization, detachment and migration of cells from the primary tumor, invasion through the basement membrane and extracellular matrix, intravasation into the blood and/or lymphatic vessels, extravasation and invasion of a target organ where cells in interaction with the microenvironment establish metastatic foci (Guan, 2015). According to this, any kind of treatment affecting this path might be of interest to combat metastatic diseases. Pretreatment with subtoxic doses of IXN, which did not decrease cell proliferation, markedly down-regulated several of these steps at the same time. Thus, the adhesiveness to plastic and Matrigel, migration, and invasion of B16-F10 cells were strongly reduced. It was recently reported that IXN exerted strong antiangiogenic effect through down-regulation of capillary-like tubule appearances on Matrigel (Serwe et al., 2012). Similarly, XN and IXN, but not 8-PN, promoted antiangiogenic and antiinflammatory effects on vascular cells (Negrão et al., 2010). Further, XN compromised adherence of MCF-7 cells to lymphendothelial cells through decreased ICAM-1 expression and epithelial-to-mesenchymal transition and cell mobility interfering with paxillin, MCL2, and S100A4 (Viola et al., 2013). Together with results presented in this study, it is indicative that hop-derived prenylflavonoids may possess the features that allow them to significantly inhibit metastatic properties of malignant cells.

Cytoskeletal proteins form a kind of matrix which statically and dynamically defines cell shape and behavior. The communication of cytoplasmic cytoskeletal proteins with the extracellular matrix is regulated through intimal contacts of specific adaptor proteins which enable their adequate response to membrane receptor stimulation (Nagano et al., 2012). Expression of integrin α-6 is one of the main characteristics of advanced carcinomas (Kacsinta et al., 2014). This protein belongs to a group of transmembrane proteins that assist cell adhesion, inter- and intracellular communication and present ECM receptors. Its expression is enhanced by VEGF and FGF. It is known that both factors are proangiogenic and are important for initial steps of neovascularization (Lee et al., 2006). Furthermore, the specific blockade of the α6β1 complex prevented the attachment of B16-BL6 cells to laminin (Ramos et al., 1990). Also, administration of EA-1, an antibody to integrin α-6, before or simultaneously with the melanoma cells, prevented the formation of metastases *in vivo* (Ruiz et al., 1993). In the present study, IXN strongly suppressed the expression of integrin α-6 that might have repercussions on almost every step in metastatic process from the adhesion to ECM, angiogenesis, and extravasation to final destination. In addition to this, knowing that integrin α-6 is expressed in stem cells (Lathia et al., 2010), the influence of IXN on its expression might reflect in a loss of “stemness” that would multiply the beneficial effect in advanced tumor treatments (Krajnović et al., 2016).

Focal adhesion kinase (FAK) has an essential role in transmitting integrin mediated signals through coupling the adaptor proteins with actin filaments during cell migration (Nagano et al., 2012). Enhanced FAK expression in human melanoma cells was found to be in correlation with aggressive forms of melanomas, but also with other types of tumors (Hess et al., 2005; Hess and Hendrix, 2006). Like other biological phenomena, FAK expression is not always in positive correlation with a metastatic process. It was shown that decreased FAK activity in B16-F10 melanoma cells increased invadopodia generation and subsequent invasion through Matrigel while migration was diminished (Kolli-Bouhafs et al., 2014). Recently, Pei et al. confirmed the significance of FAK expression in the regulation of main signaling pathways as well as gene expression involved in the regulation of B16-F10 and A375 cell migration/metastasis (Pei et al., 2017). Many flavonoids (e.g. galangin, genistein, quercetin, luteolin, etc.) are able to interfere with FAK activity, affecting the metastatic process (Cui et al., 2017; Huang et al., 2005; Zhang et al., 2013). In addition, in prostate cancer, XN-mediated inhibition of FAK was found to be beneficial (Venè et al., 2012). Reduced FAK, AKT, and NF-κB levels resulted following XN exposure, and promoted a less invasive phenotype of ALL cells (Benelli et al., 2012). Accordingly, a diminished expression of FAK upon the exposure of B16-

F10 cells to IXN was found. This result is in concordance with down-regulated α-6 integrin and subsequent Rho expression. Rho family GTPases are connected with numerous proteins involved in the regulation of intracellular actin dynamic and cell movement of different cancer types including melanoma (Sanz-Moreno and Marshall, 2009). The application of Rho kinase inhibitors abrogated melanoma cell invasion, damaging “amoeboid-like" and mesenchymal-like modes of invasion in culture (Sadok et al., 2015). Inhibition of FAK could be related to Rho kinase inhibition in response to an IXN stimulus, since it has been reported that FAK binds to Rho GEF which is responsible for further Rho A and C activation (Miller et al., 2014). Vinculin possesses a very important role in linking focal adhesion with the actin cytoskeleton. IXN potential to decrease vinculin and also β-Actin expression might be an additional factor responsible for decreased metastatic features of treated B16-F10 cells (Bays and DeMali, 2017). β-Actin is ubiquitously expressed and usually serves as a reference for protein expression evaluation. However, some literature data show that it is up-regulated in numerous cancers like melanoma, liver, renal, colorectal, gastric, pancreatic, esophageal, lung, breast, prostate, ovarian cancers, leukemia, and lymphoma (Guo et al., 2013). The abnormal expression and polymerization of β-actin and consequent cytoskeleton alteration are related to the establishment of an invasive phenotype. In contrast to other actin family members, α-Smooth muscle actin (α-SMA) is restricted to cells of the smooth muscle lineage but it is typical for particular fibroblasts known as miofibroblasts, hepatic perisinusoidal cells, pericytes, and myoepithelial cells (Rockey et al., 2013). In cancer tissues, its expression is ascribed to cancer-associated fibroblasts and considered a prognostic marker indicative for a bad ethiopathologies. Therefore, α-SMA positive myofibroblasts correlate with worse overall survival of patients with invasive breast or pancreatic cancer and melanoma (Nanda, 2010; Tsukamoto et al., 1992; Yamashita et al., 2012). There are just a few recorded cases about α-SMA expression in tumor cells. α-Smooth muscle actin is involved in migration, invasion, transendothelial penetration of lung adenocarcinoma cells while its neutralization abolished their stemness (Lee et al., 2013). Additionally, its expression is evidenced in one case of benign schwannoma, one primary cutaneous melanoma, and four melanomas, all tumors originating from neural crest (Dundr et al., 2009). The presence of α-SMA indicated their low differentiated phenotype and impressive plasticity since it was found that CAF possessed the same genetic abnormalities as tumor bulk cells (Nair et al., 2017). Thus, IXN potential to reduce the expression of this molecule presents a very valuable result and emphasizes its importance in eliminating or transforming the stem phenotype.

Taking into account all mentioned activities of IXN against metastatic B16-F10 clone it was not surprising that the number and diameter of metastatic nodules in the lungs of animals exposed to the compound for more than 2 weeks were remarkably lower in comparison to untreated animals. The decreased expression of HMGB1 in IXN treated animals might be beneficial in terms that this molecule is considered as a marker of cancer progression (Li et al., 2014). It was shown that HMGB1 overexpression is associated with all cancer hallmarks, including invasion and metastasis (Tang et al., 2010). More precisely, Huber et al. found that enhanced expression of HMGB1 was in correlation with the progression and metastasis development in murine B16 melanoma model while increased serum concentration of this protein was detected in patients with metastatic melanoma. In addition to direct influence on tumor cells, HMGB1 might induce reprogram of innate immune cells toward protumorigenic phenotype (Huber et al., 2016). On the other hand, the presence of S100 positive spindle shape cells and absence of Ki-67 expression in metastatic lesions of animals treated with IXN indicated that melanoma cells underwent the process of differentiation. S100 protein family comprises of many different proteins that are present in numerous types of cells, including melanocytes and cells of tumors of epithelial origin (Petersson et al., 2009). They are responsible for many important aspects of cellular physiology like proliferation, differentiation, apoptosis, inflammation, and migration/invasion (Donato et al., 2013). Even if, at the moment, we are not able to exclude differential expression and functions of separated members of this family, the increased expression of S100 in lungs of IXN treated animals can at least confirm that the cells with changed morphology are definitely melanoma cells with diminished dividing potential.

Keeping in mind the data previously published by our group (Krajnović et al., 2016) showing the beneficial effect of IXN in a model of solid melanoma, the potential of this naturally occurring food compound should be considered for future investigations as differentiation-inducing, chemo-sensitizing, and antimetastatic agent.

Conflict of interest

None.

Acknowledgements

The authors from University of Belgrade acknowledge financial support from the Ministry of Education, Science and Technological Development of the Republic of Serbia (Grant No. 173013) and the Leibniz Institute of Plant Biochemistry, Halle, from the German Academic Exchange Service (DAAD), as well as support from Hopsteiner (Simon H. Steiner Hopfen GmbH). We thank Martina Lerbs (IPB) for technical assistance, Dr. Jasmina Živanović for the assistance with the fluorescence microscopy and Mrs. Jasmina Ninkov, B.Sc. in English Language and Literature, Commissioned Scientific and Technical Translator, for proof reading of the entire manuscript.

Appendix A. Supplementary data

Supplementary data to this article can be found online at https://doi.org/10.1016/j.fct.2019.04.046.

References

Allsopp, P., Possemiers, S., Campbell, D., Gill, C., Rowland, I., 2013. A comparison of the anticancer properties of isoxanthohumol and 8-prenylnaringenin using in vitro models of colon cancer. Biofactors 39, 441–447. https://doi.org/10.1002/biof.1084.

Anand, P., Kunnumakkara, A.B., Kunnumakara, A.B., Sundaram, C., Harikumar, K.B., Tharakan, S.T., Lai, O.S., Sung, B., Aggarwal, B.B., 2008. Cancer is a preventable disease that requires major lifestyle changes. Pharm. Res. (N. Y.) 25, 2097–2116. https://doi.org/10.1007/s11095-008-9661-9.

Balint, K., Xiao, M., Pinnix, C.C., Soma, A., Veres, I., Juhasz, I., Brown, E.J., Capobianco, A.J., Herlyn, M., Liu, Z.-J., 2005. Activation of Notch1 signaling is required for beta-catenin-mediated human primary melanoma progression. J. Clin. Investig. 115, 3166–3176. https://doi.org/10.1172/JCI25001.

Bays, J.L., DeMali, K.A., 2017. Vinculin in cell–cell and cell–matrix adhesions. Cell. Mol. Life Sci. 74, 2999–3009. https://doi.org/10.1007/s00018-017-2511-3.

Benelli, R., Venè, R., Ciarlo, M., Carlone, S., Barbieri, O., Ferrari, N., 2012. The AKT/NF-κB inhibitor xanthohumol is a potent anti-lymphocytic leukemia drug overcoming chemoresistance and cell infiltration. Biochem. Pharmacol. 83, 1634–1642. https://doi.org/10.1016/j.bcp.2012.03.006.

Bertl, E., Becker, H., Eicher, T., Herhaus, C., Kapadia, G., Bartsch, H., Gerhäuser, C., 2004a. Inhibition of endothelial cell functions by novel potential cancer chemopreventive agents. Biochem. Biophys. Res. Commun. 325, 287–295. https://doi.org/10.1016/j.bbrc.2004.10.032.

Bertl, E., Klimo, K., Heiss E, E., Klenke, F., Peschke, P., Becker, H., Eicher, T., Herhaus, C., Kapadia, G., Bartsch, H., C.G, 2004b. Identification of novel inhibitors of angiogenesis using a human in vitro anti-angiogenic assay (pp. 47-61). Int. J. Cancer Res. Prev. 47–61.

Borrull, A., Ghislin, S., Deshayes, F., Lauriol, J., Alcaide-Loridan, C., Middendorp, S., 2012. Nanog and Oct4 overexpression increases motility and transmigration of melanoma cells. J. Cancer Res. Clin. Oncol. 138, 1145–1154. https://doi.org/10.1007/s00432-012-1186-2.

Cui, S., Wang, J., Wu, Q., Qian, J., Yang, C., Bo, P., 2017. Genistein inhibits the growth and regulates the migration and invasion abilities of melanoma cells via the FAK/paxillin and MAPK pathways. Oncotarget 8, 21674–21691. https://doi.org/10.18632/oncotarget.15535.

Damsky, W.E., Curley, D.P., Santhanakrishnan, M., Rosenbaum, L.E., Platt, J.T., Gould Rothberg, B.E., Taketo, M.M., Dankort, D., Rimm, D.L., McMahon, M., Bosenberg, M., 2011. β-catenin signaling controls metastasis in Braf-activated Pten-deficient melanomas. Cancer Cell 20, 741–754. https://doi.org/10.1016/j.ccr.2011.10.030.

Danciu, C., Falamas, A., Dehelean, C., Soica, C., Radeke, H., Barbu-Tudoran, L., Bojin, F., Pînzaru, S., Munteanu, M.F., 2013. A characterization of four B16 murine melanoma

cell sublines molecular fingerprint and proliferation behavior. Cancer Cell Int. 13, 75. https://doi.org/10.1186/1475-2867-13-75.
Delmulle, L., Bellahcène, A., Dhooge, W., Comhaire, F., Roelens, F., Huvaere, K., Heyerick, A., Castronovo, V., De Keukeleire, D., 2006. Anti-proliferative properties of prenylated flavonoids from hops (Humulus lupulus L.) in human prostate cancer cell lines. Phytomedicine 13, 732–734. https://doi.org/10.1016/j.phymed.2006.01.001.
Delmulle, L., Vanden Berghe, T., Keukeleire, D. De, Vandenabeele, P., 2008. Treatment of PC-3 and DU145 prostate cancer cells by prenylflavonoids from hop (Humulus lupulus L.) induces a caspase-independent form of cell death. Phytother Res. 22, 197–203. https://doi.org/10.1002/ptr.2286.
Donato, R., Cannon, B.R., Sorci, G., Riuzzi, F., Hsu, K., Weber, D.J., Geczy, C.L., 2013. Functions of S100 proteins. Curr. Mol. Med. 13, 24–57.
Drenzek, J.G., Seiler, N.L., Jaskula-Sztul, R., Rausch, M.M., Rose, S.L., 2011. Xanthohumol decreases Notch1 expression and cell growth by cell cycle arrest and induction of apoptosis in epithelial ovarian cancer cell lines. Gynecol. Oncol. 122, 396–401. https://doi.org/10.1016/j.ygyno.2011.04.027.
Dundr, P., Povýsil, C., Tvrdík, D., 2009. Actin expression in neural crest cell-derived tumors including schwannomas, malignant peripheral nerve sheath tumors, neurofibromas and melanocytic tumors. Pathol. Int. 59, 86–90. https://doi.org/10.1111/j.1440-1827.2008.02333.x.
Farag, M.A., Wessjohann, L.A., 2013. Cytotoxic effect of commercial Humulus lupulus L. (hop) preparations - in comparison to its metabolomic fingerprint. J. Adv. Res. 4, 417–421. https://doi.org/10.1016/j.jare.2012.07.006.
Farag, M.A., Porzel, A., Schmidt, J., Wessjohann, L.A., 2012. Metabolite profiling and fingerprinting of commercial cultivars of Humulus lupulus L. (hop): a comparison of MS and NMR methods in metabolomics. Metabolomics 8, 492–507. https://doi.org/10.1007/s11306-011-0335-y.
Farag, M.A., Mahrous, E.A., Lübken, T., Porzel, A., Wessjohann, L., 2014. Classification of commercial cultivars of Humulus lupulus L. (hop) by chemometric pixel analysis of two dimensional nuclear magnetic resonance spectra. Metabolomics 10, 21–32. https://doi.org/10.1007/s11306-013-0547-4.
Flaherty, K.T., Puzanov, I., Kim, K.B., Ribas, A., McArthur, G.A., Sosman, J.A., O'Dwyer, P.J., Lee, R.J., Grippo, J.F., Nolop, K., Chapman, P.B., 2010. Inhibition of mutated, activated BRAF in metastatic melanoma. N. Engl. J. Med. 363, 809–819. https://doi.org/10.1056/NEJMoa1002011.
Gerhäuser, C., 2005. Beer constituents as potential cancer chemopreventive agents. Eur. J. Cancer 41, 1941–1954. https://doi.org/10.1016/j.ejca.2005.04.012.
Guan, X., 2015. Cancer metastases: challenges and opportunities. Acta Pharm. Sin. B 5, 402–418. https://doi.org/10.1016/j.apsb.2015.07.005.
Guo, C., Liu, S., Wang, J., Sun, M.-Z., Greenaway, F.T., 2013. ACTB in cancer. Clin. Chim. Acta 417, 39–44. https://doi.org/10.1016/j.cca.2012.12.012.
Hanahan, D., Weinberg, R.A., 2011. Hallmarks of cancer: the next generation. Cell 144, 646–674. https://doi.org/10.1016/j.cell.2011.02.013.
Hauschild, A., Grob, J.-J., Demidov, L.V., Jouary, T., Gutzmer, R., Millward, M., Rutkowski, P., Blank, C.U., Miller, W.H., Kaempgen, E., Martín-Algarra, S., Karaszewska, B., Mauch, C., Chiarion-Sileni, V., Martin, A.-M., Swann, S., Haney, P., Mirakhur, B., Guckert, M.E., Goodman, V., Chapman, P.B., 2012. Dabrafenib in BRAF-mutated metastatic melanoma: a multicentre, open-label, phase 3 randomised controlled trial. Lancet 380, 358–365. https://doi.org/10.1016/S0140-6736(12)60868-X.
Hess, A.R., Hendrix, M.J.C., 2006. Focal adhesion kinase signaling and the aggressive melanoma phenotype. Cell Cycle 5, 478–480. https://doi.org/10.4161/cc.5.5.2518.
Hess, A.R., Postovit, L.-M., Margaryan, N.V., Seftor, E.A., Schneider, G.B., Seftor, R.E.B., Nickoloff, B.J., Hendrix, M.J.C., 2005. Focal adhesion kinase promotes the aggressive melanoma phenotype. Cancer Res. 65, 9851–9860. https://doi.org/10.1158/0008-5472.CAN-05-2172.
Hodi, F.S., O'Day, S.J., McDermott, D.F., Weber, R.W., Sosman, J.A., Haanen, J.B., Gonzalez, R., Robert, C., Schadendorf, D., Hassel, J.C., Akerley, W., van den Eertwegh, A.J.M., Lutzky, J., Lorigan, P., Vaubel, J.M., Linette, G.P., Hogg, D., Ottensmeier, C.H., Lebbé, C., Peschel, C., Quirt, I., Clark, J.I., Wolchok, J.D., Weber, J.S., Tian, J., Yellin, M.J., Nichol, G.M., Hoos, A., Urba, W.J., 2010. Improved survival with ipilimumab in patients with metastatic melanoma. N. Engl. J. Med. 363, 711–723. https://doi.org/10.1056/NEJMoa1003466.
Huang, Y.T., Lee, L.T., Lee, P.P.H., Lin, Y.S., Lee, M.T., 2005. Targeting of focal adhesion kinase by flavonoids and small-interfering RNAs reduces tumor cell migration ability. Anticancer Res. 25, 2017–2025.
Huber, R., Meier, B., Otsuka, A., Fenini, G., Satoh, T., Gehrke, S., Widmer, D., Levesque, M.P., Mangana, J., Kerl, K., Gebhardt, C., Fujii, H., Nakashima, C., Nonomura, Y., Kabashima, K., Dummer, R., Contassot, E., French, L.E., 2016. Tumour hypoxia promotes melanoma growth and metastasis via High Mobility Group Box-1 and M2-like macrophages. Sci. Rep. 6, 29914. https://doi.org/10.1038/srep29914.
Hudcová, T., Bryndová, J., Fialová, K., Fiala, J., Karabín, M., Jelínek, L., Dostálek, P., 2014. Antiproliferative effects of prenylflavonoids from hops on human colon cancer cell lines. J. Inst. Brew. 120, 225–230. https://doi.org/10.1002/jib.139.
Jin, J.H., Kim, J.S., Kang, S.S., Son, K.H., Chang, H.W., Kim, H.P., 2010. Anti-inflammatory and anti-arthritic activity of total flavonoids of the roots of Sophora flavescens. J. Ethnopharmacol. 127, 589–595. https://doi.org/10.1016/j.jep.2009.12.020.
Kacsinta, A.D., Rubenstein, C.S., Sroka, I.C., Pawar, S., Gard, J.M., Nagle, R.B., Cress, A.E., 2014. Intracellular modifiers of integrin alpha 6p production in aggressive prostate and breast cancer cell lines. Biochem. Biophys. Res. Commun. 454, 335–340. https://doi.org/10.1016/j.bbrc.2014.10.073.
Kolli-Bouhafs, K., Sick, E., Noulet, F., Gies, J.-P., De Mey, J., Rondé, P., 2014. FAK competes for Src to promote migration against invasion in melanoma cells. Cell Death Dis. 5, e1379. https://doi.org/10.1038/cddis.2014.329.
Krajnović, T., Kaluđerović, G.N., Wessjohann, L.A., Mijatović, S., Maksimović-Ivanić, D., 2016. Versatile antitumor potential of isoxanthohumol: enhancement of paclitaxel activity in vivo. Pharmacol. Res. 105, 62–73. https://doi.org/10.1016/j.phrs.2016.01.011.
Kunnimalaiyaan, S., Sokolowski, K.M., Balamurugan, M., Gamblin, T.C., Kunnimalaiyaan, M., 2015a. Xanthohumol inhibits Notch signaling and induces apoptosis in hepatocellular carcinoma. PLoS One 10, e0127464. https://doi.org/10.1371/journal.pone.0127464.
Kunnimalaiyaan, S., Trevino, J., Tsai, S., Gamblin, T.C., Kunnimalaiyaan, M., 2015b. Xanthohumol-mediated suppression of Notch1 signaling is associated with antitumor activity in human pancreatic cancer cells. Mol. Canc. Therapeut. 14, 1395–1403. https://doi.org/10.1158/1535-7163.MCT-14-0915.
Lathia, J.D., Gallagher, J., Heddleston, J.M., Wang, J., Eyler, C.E., MacSwords, J., Wu, Q., Vasanji, A., McLendon, R.E., Hjelmeland, A.B., Rich, J.N., 2010. Integrin alpha 6 regulates glioblastoma stem cells. Cell Stem Cell 6, 421–432. https://doi.org/10.1016/j.stem.2010.02.018.
Lee, T.-H., Seng, S., Li, H., Kennel, S.J., Avraham, H.K., Avraham, S., 2006. Integrin regulation by vascular endothelial growth factor in human brain microvascular endothelial cells: role of alpha6beta1 integrin in angiogenesis. J. Biol. Chem. 281, 40450–40460. https://doi.org/10.1074/jbc.M607525200.
Lee, S.H., Kim, H.J., Lee, J.S., Lee, I.-S., Kang, B.Y., 2007. Inhibition of topoisomerase I activity and efflux drug transporters' expression by xanthohumol. from hops. Arch Pharm. Res. (Seoul) 30, 1435–1439.
Lee, H.W., Park, Y.M., Lee, S.J., Cho, H.J., Kim, D.-H., Lee, J.-I., Kang, M.-S., Seol, H.J., Shim, Y.M., Nam, D.-H., Kim, H.H., Joo, K.M., 2013. Alpha-smooth muscle actin (ACTA2) is required for metastatic potential of human lung adenocarcinoma. Clin. Cancer Res. 19, 5879–5889. https://doi.org/10.1158/1078-0432.CCR-13-1181.
Li, Q., Li, J., Wen, T., Zeng, W., Peng, C., Yan, S., Tan, J., Yang, K., Liu, S., Guo, A., Zhang, C., Su, J., Jiang, M., Liu, Z., Zhou, H., Chen, X., 2014. Overexpression of HMGB1 in melanoma predicts patient survival and suppression of HMGB1 induces cell cycle arrest and senescence in association with p21 (Waf1/Cip1) up-regulation via a p53-independent, Sp1-dependent pathway. Oncotarget 5, 6387–6403. https://doi.org/10.18632/oncotarget.2201.
Liu, M., Hansen, P.E., Wang, G., Qiu, L., Dong, J., Yin, H., Qian, Z., Yang, M., Miao, J., 2015. Pharmacological profile of xanthohumol, a prenylated flavonoid from hops (Humulus lupulus). Molecules 20, 754–779. https://doi.org/10.3390/molecules20010754.
Liu, M., Zhang, W., Zhang, W., Zhou, X., Li, M., Miao, J., 2017. Prenylflavonoid isoxanthohumol sensitizes MCF-7/ADR cells to doxorubicin cytotoxicity via acting as a substrate of ABCB1. Toxins 9, 208. https://doi.org/10.3390/toxins9070208.
Miller, N.L.G., Kleinschmidt, E.G., Schlaepfer, D.D., 2014. RhoGEFs in cell motility: novel links between Rgnef and focal adhesion kinase. Curr. Mol. Med. 14, 221–234.
Miranda, C.L., Stevens, J.F., Helmrich, A., Henderson, M.C., Rodriguez, R.J., Yang, Y.H., Deinzer, M.L., Barnes, D.W., Buhler, D.R., 1999. Antiproliferative and cytotoxic effects of prenylated flavonoids from hops (Humulus lupulus) in human cancer cell lines. Food Chem. Toxicol. 37, 271–285.
Mojic, M., Mijatovic, S., Maksimovic-Ivanic, D., Miljkovic, D., Stosic-Grujicic, S., Stankovic, M., Mangano, K., Travali, S., Donia, M., Fagone, P., Zocca, M.-B., Al-Abed, Y., McCubrey, J.A., Nicoletti, F., 2012. Therapeutic potential of nitric oxide-modified drugs in colon cancer cells. Mol. Pharmacol. 82, 700–710. https://doi.org/10.1124/mol.112.077842.
Monteiro, R., Faria, A., Azevedo, I., Calhau, C., 2007. Modulation of breast cancer cell survival by aromatase inhibiting hop (Humulus lupulus L.) flavonoids. J. Steroid Biochem. Mol. Biol. 105, 124–130. https://doi.org/10.1016/j.jsbmb.2006.11.026.
Monteiro, R., Calhau, C., Silva, A.O.E., Pinheiro-Silva, S., Guerreiro, S., Gärtner, F., Azevedo, I., Soares, R., 2008. Xanthohumol inhibits inflammatory factor production and angiogenesis in breast cancer xenografts. J. Cell. Biochem. 104, 1699–1707. https://doi.org/10.1002/jcb.21738.
Nagano, M., Hoshino, D., Koshikawa, N., Akizawa, T., Seiki, M., 2012. Turnover of focal adhesions and cancer cell migration. Int. J. Cell Biol. 1–10. 2012. https://doi.org/10.1155/2012/310616.
Nair, N., Calle, A.S., Zahra, M.H., Prieto-Vila, M., Oo, A.K.K., Hurley, L., Vaidyanath, A., Seno, A., Masuda, J., Iwasaki, Y., Tanaka, H., Kasai, T., Seno, M., 2017. A cancer stem cell model as the point of origin of cancer-associated fibroblasts in tumor microenvironment. Sci. Rep. 7, 6838. https://doi.org/10.1038/s41598-017-07144-5.
Nanda, S., 2010. High stromal expression of α-smooth-muscle actin correlates with aggressive pancreatic cancer biology. Nat. Rev. Gastroenterol. Hepatol. 7 652–652. https://doi.org/10.1038/nrgastro.2010.179.
Negrão, R., Costa, R., Duarte, D., Taveira Gomes, T., Mendanha, M., Moura, L., Vasques, L., Azevedo, I., Soares, R., 2010. Angiogenesis and inflammation signaling are targets of beer polyphenols on vascular cells. J. Cell. Biochem. 111, 1270–1279. https://doi.org/10.1002/jcb.22850.
Negrão, R., Duarte, D., Costa, R., Soares, R., 2013. Isoxanthohumol modulates angiogenesis and inflammation via vascular endothelial growth factor receptor, tumor necrosis factor alpha and nuclear factor kappa B pathways. Biofactors 39, 608–622. https://doi.org/10.1002/biof.1122.
Ortiz, R., Díaz, J., Díaz, N., Lobos-Gonzalez, L., Cárdenas, A., Contreras, P., Díaz, M.I., Otte, E., Cooper-White, J., Torres, V., Leyton, L., Quest, A.F.G., 2016. Extracellular matrix-specific Caveolin-1 phosphorylation on tyrosine 14 is linked to augmented melanoma metastasis but not tumorigenesis. Oncotarget 7, 40571–40593. https://doi.org/10.18632/oncotarget.9738.
Pei, G., Lan, Y., Chen, D., Ji, L., Hua, Z.-C., 2017. FAK regulates E-cadherin expression via p-SrcY416/p-ERK1/2/p-Stat3Y705 and PPARγ/miR-125b/Stat3 signaling pathway in B16F10 melanoma cells. Oncotarget 8, 13898–13908. https://doi.org/10.18632/oncotarget.14687.
Petersson, S., Shubbar, E., Enerbäck, L., Enerbäck, C., 2009. Expression patterns of S100 proteins in melanocytes and melanocytic lesions. Melanoma Res. 19, 215–225.

https://doi.org/10.1097/CMR.0b013e32832c6358.
Ramos, D.M., Berston, E.D., Kramer, R.H., 1990. Analysis of integrin receptors for laminin and type IV collagen on metastatic B16 melanoma cells. Cancer Res. 50, 728–734.
Rimm, D.L., Caca, K., Hu, G., Harrison, F.B., Fearon, E.R., 1999. Frequent nuclear/cytoplasmic localization of beta-catenin without exon 3 mutations in malignant melanoma. Am. J. Pathol. 154, 325–329.
Rockey, D.C., Weymouth, N., Shi, Z., 2013. Smooth muscle α actin (Acta2) and myofibroblast function during hepatic wound healing. PLoS One 8, e77166. https://doi.org/10.1371/journal.pone.0077166.
Ruiz, P., Dunon, D., Sonnenberg, A., Imhof, B.A., 1993. Suppression of mouse melanoma metastasis by EA-1, a monoclonal antibody specific for alpha 6 integrins. Cell Adhes. Commun. 1, 67–81.
Sadok, A., McCarthy, A., Caldwell, J., Collins, I., Garrett, M.D., Yeo, M., Hooper, S., Sahai, E., Kuemper, S., Mardakheh, F.K., Marshall, C.J., 2015. Rho kinase inhibitors block melanoma cell migration and inhibit metastasis. Cancer Res. 75, 2272–2284. https://doi.org/10.1158/0008-5472.CAN-14-2156.
Sandru, A., Voinea, S., Panaitescu, E., Blidaru, A., 2014. Survival rates of patients with metastatic malignant melanoma. J. Med. Life 7, 572–576.
Sanz-Moreno, V., Marshall, C.J., 2009. Rho-GTPase signaling drives melanoma cell plasticity. Cell Cycle 8, 1484–1487. https://doi.org/10.4161/cc.8.10.8490.
Serwe, A., Rudolph, K., Anke, T., Erkel, G., 2012. Inhibition of TGF-β signaling, vasculogenic mimicry and proinflammatory gene expression by isoxanthohumol. Investig. New Drugs 30, 898–915. https://doi.org/10.1007/s10637-011-9643-3.
Shalini, S., Dorstyn, L., Dawar, S., Kumar, S., 2015. Old, new and emerging functions of caspases. Cell Death Differ. 22, 526–539. https://doi.org/10.1038/cdd.2014.216.
Stevens, J.F., Page, J.E., 2004. Xanthohumol and related prenylflavonoids from hops and beer: to your good health!. Phytochemistry 65, 1317–1330. https://doi.org/10.1016/j.phytochem.2004.04.025.
Stompor, M., Świtalska, M., Podgórski, R., Uram, Ł., Aebisher, D., Wietrzyk, J., 2017. Synthesis and biological evaluation of 4'-O-acetyl-isoxanthohumol and its analogues as antioxidant and antiproliferative agents. Acta Biochim. Pol. 64, 577–583. https://doi.org/10.18388/abp.2017_1608.
Tan, K.W., Cooney, J., Jensen, D., Li, Y., Paxton, J.W., Birch, N.P., Scheepens, A., 2014. Hop-derived prenylflavonoids are substrates and inhibitors of the efflux transporter breast cancer resistance protein (BCRP/ABCG2). Mol. Nutr. Food Res. 58, 2099–2110. https://doi.org/10.1002/mnfr.201400288.
Tang, D., Kang, R., Zeh III, H.J., Lotze, M.T., 2010. High-mobility group box 1 and cancer. Biochim. Biophys. Acta - Gene Regul. Mech. 1799, 131–140. https://doi.org/10.1016/j.bbagrm.2009.11.014.
Tronina, T., Bartmańska, A., Filip-Psurska, B., Wietrzyk, J., Popłoński, J., Huszcza, E., 2013. Fungal metabolites of xanthohumol with potent antiproliferative activity on human cancer cell lines in vitro. Bioorg. Med. Chem. 21 2001–6. https://doi.org/10.1016/j.bmc.2013.01.026.
Tsukamoto, H., Mishima, Y., Hayashibe, K., Sasase, A., 1992. Alpha-smooth muscle actin expression in tumor and stromal cells of benign and malignant human pigment cell tumors. J. Investig. Dermatol. 98, 116–120.
Venè, R., Benelli, R., Minghelli, S., Astigiano, S., Tosetti, F., Ferrari, N., 2012. Xanthohumol impairs human prostate cancer cell growth and invasion and diminishes the incidence and progression of advanced tumors in TRAMP mice. Mol. Med. 18, 1292–1302. https://doi.org/10.2119/molmed.2012.00174.
Venturelli, S., Burkard, M., Biendl, M., Lauer, U.M., Frank, J., Busch, C., 2016. Prenylated chalcones and flavonoids for the prevention and treatment of cancer. Nutrition 32, 1171–1178. https://doi.org/10.1016/j.nut.2016.03.020.
Vineis, P., Wild, C.P., 2014. Global cancer patterns: causes and prevention. Lancet 383, 549–557. https://doi.org/10.1016/S0140-6736(13)62224-2.
Viola, K., Kopf, S., Rarova, L., Jarukamjorn, K., Kretschy, N., Teichmann, M., Vonach, C., Atanasov, A.G., Giessrigl, B., Huttary, N., Raab, I., Krieger, S., Strnad, M., de Martin, R., Saiko, P., Szekeres, T., Knasmüller, S., Dirsch, V.M., Jäger, W., Grusch, M., Dolznig, H., Mikulits, W., Krupitza, G., 2013. Xanthohumol attenuates tumour cell-mediated breaching of the lymphendothelial barrier and prevents intravasation and metastasis. Arch. Toxicol. 87, 1301–1312. https://doi.org/10.1007/s00204-013-1028-2.
Wilhelm, H., Wessjohann, L.A., 2006. An efficient synthesis of the phytoestrogen 8-prenylnaringenin from xanthohumol by a novel demethylation process. Tetrahedron 62, 6961–6966. https://doi.org/10.1016/J.TET.2006.04.060.
Yamashita, M., Ogawa, T., Zhang, X., Hanamura, N., Kashikura, Y., Takamura, M., Yoneda, M., Shiraishi, T., 2012. Role of stromal myofibroblasts in invasive breast cancer: stromal expression of alpha-smooth muscle actin correlates with worse clinical outcome. Breast Canc. 19, 170–176. https://doi.org/10.1007/s12282-010-0234-5.
Yang, J.-Y., Della-Fera, M.A., Rayalam, S., Baile, C.A., 2007. Effect of xanthohumol and isoxanthohumol on 3T3-L1 cell apoptosis and adipogenesis. Apoptosis 12, 1953–1963. https://doi.org/10.1007/s10495-007-0130-4.
Zhang, W., Tang, B., Huang, Q., Hua, Z., 2013. Galangin inhibits tumor growth and metastasis of B16F10 melanoma. J. Cell. Biochem. 114, 152–161. https://doi.org/10.1002/jcb.24312.
Zołnierczyk, A.K., Mączka, W.K., Grabarczyk, M., Wińska, K., Woźniak, E., Anioł, M., 2015. Isoxanthohumol - biologically active hop flavonoid. Fitoterapia 103, 71–82. https://doi.org/10.1016/j.fitote.2015.03.007.